minerals

MDPI

Article

Separation Mechanism of Fatty Acids from Waste Cooking Oil and Its Flotation Performance in Iron Ore Desiliconization

Wenda Guo [1,*], Yimin Zhu [1,*], Yuexin Han [1], Yihe Wei [2] and Binbin Luo [1]

[1] College of Resource and Civil Engineering, Northeastern University, Shenyang 110819, China; dongdafulong@mail.neu.edu.cn (Y.H.); bluo2@ualberta.ca (B.L.)
[2] College of Resource and Civil Engineering, Wuhan Institute of Technology, Wuhan 430073, China; yhwei@wit.edu.cn
* Correspondence: gedaya123@163.com (W.G.); zhuyimin@mail.neu.edu.cn (Y.Z.); Tel.: +86-24-8367-6828 (W.G.)

Received: 16 October 2017; Accepted: 5 December 2017; Published: 12 December 2017

Abstract: Using the mixed fatty acids (MFA) produced by waste cooking oil as flotation collectors directly, the flotation effect is usually not satisfactory, especially at lower temperature, which may be due to the presence of large amounts of saturated fatty acids. In this study, waste cooking oil was separated into saturated fatty acids (SFA) and unsaturated fatty acids (UFA). The separation mechanism was studied by molecular simulation based on quantum and molecular mechanics. SFA and UFA were analyzed by iodine value, melting point measurement and Fourier transform infrared (FT-IR) spectroscopy to check the result of the separation. The micro-flotation and bench-scale flotation tests were performed to investigate the flotation differences between SFA and UFA. The results showed that the poor flotation performance of waste cooking oil was due to the large amount of SFA in presence. If the SFA was separated out, the TFe grade and recovery of the flotation concentrates would be increased by 4.09 and 2.70 percentage points, respectively and the SiO_2 grade would be 4.03 percentage points lower at the same time. This study would provide technical supports and theoretical guidance for the waste cooking oil application in the field of mineral processing.

Keywords: waste cooking oil; fatty acids; separation; flotation performance

1. Introduction

Waste cooking oil refers to vegetable oil and animal fat losing food value and the wastes of oil deep processing [1]. With the continuous development of economy and society, the scale of catering industry is expanding fast and resulting in a significant increase in the discharge of waste cooking oil [2]. As a large edible oil consumption country, it's estimated that China has produced considerable amount of waste cooking oil annually (about 8–15 million tons) and half of them could be collected for recycling [3,4]. However, waste cooking oil is not satisfactorily recycled for industry use in the past years, as 40%–60% is back flow to dining tables through various illegal channels [5] and the rest is mostly disposed as rubbish. The main chemical composition of waste cooking oil is the higher fatty acid glyceride [6], which can be used to produce anionic fatty acids for mineral flotation. China's oxide ore flotation industry requires more than 800 thousand tons fatty acid collector every year. The traditional process of preparing fatty acids mainly through chemical synthesis [7]. With the increase in industrial costs, the new material choices such as waste cooking oil to prepare fatty acids will increasingly receive attention.

Quartz is one of the most widely distributed minerals on the surface of the earth [8], which is the most common gangue minerals associated with oxides, sulfides, silicates and phosphates [9,10].

Flotation is the main measure of separating quartz and two typical methods are used, the one is directly flotation with cationic amine collectors, the other is activated by the polyvalent metal ions and then using anionic collectors for reverse flotation [11–13]. In China, due to plentiful raw material sources and lower production costs, most concentrators choose fatty acid collectors to reverse float quartz for the desiliconization of iron ores [14,15]. For example, RA series collectors (RA-315, RA-515, RA-715 and RA-915) prepared by fatty acids and characterized by good properties of low cost and non-toxicity have been used for reverse flotation of iron ores for many years in China [16–18]. However, using the mixed fatty acids produced by waste cooking oil as flotation collectors directly, the flotation effect is usually not satisfactory, especially at lower temperature or room temperature. Some researchers have tried to improve the problem by mixing with other surfactants but the collector dosage is quite large and the cost is also high [19–21], thus severely limiting the use of waste cooking oil for minerals flotation. In this study, a new method is proposed to explore and fundamentally solve the problem of the poor low-temperature flotation performance of waste cooking oil by the separation of different fatty acids.

The chemical constituents of the waste cooking oil fatty acids are saturated fatty acids (SFA) such as stearic acid and palmitic acid and unsaturated fatty acids (UFA) such as oleic acid, linoleic acid and linolenic acid [22]. Some researchers have revealed that the unsaturation degree of fatty acids is greatly related to their flotation properties [23–25]. Saturated fatty acids such as stearic acid and palmitic acid have bad floatability and selectivity and do not easily foam in the flotation process [24,25]. While unsaturated fatty acids proved to be an excellent collector suitable for low temperature and as the degree of unsaturation increases, low temperature flotation performance is enhanced [23]. Under certain conditions, urea can form crystalline compounds with linear fatty acids containing 6 more carbon atoms, which can be used to separate SFA and UFA [26–28]. With this method, it is possible to separate out the SFA from waste cooking oil to strength its low temperature flotation performance. Finally, the problems of large amount of collector, high flotation temperature and poor flotation index when using waste cooking oil as flotation collector would be solved by the separation of different fatty acids.

In this work, the waste cooking oil was separated into SFA and UFA. The separation mechanism was innovatively studied by molecular simulation based on quantum mechanics and molecular mechanics. Dissolution characteristics, the degree of unsaturation and the molecular properties of SFA and UFA were analyzed by iodine value, melting point and infrared spectroscopy to check the separation effect of different types fatty acids from waste cooking oil. Then, the flotation performance differences of SFA and UFA were investigated by series micro-flotation tests of quartz. Based on results of micro-flotation tests, bench-scale flotation tests were performed with industrial iron ores to further investigate the desilication performance of UFA and SFA. The scanning electron microscope with an attached EDS microanalyzer (SEM/EDS) and X-ray diffraction were used to investigate the characteristics of bench-scale flotation tailings and the desilication efficiency of UFA and SFA.

2. Materials and Methods

2.1. Mineral

The carefully hand-picked pure quartz samples from the Sijiaying iron mine, Tangshan, China, were first crushed with hammer, then grinded in a porcelain mill with agate balls and wet-sieved to obtain the −0.074 mm size fractions for micro-flotation tests. The chemical compositions and X-ray diffraction (XRD) (PW3040, PANalytical B.V., Almero, The Netherlands) analyses of the obtained quartz sample were presented in Table 1 and Figure 1a, respectively. The quartz sample consists of 99.20% (wt %) SiO_2, which meets the desirable requirement of purity for the experiments.

Table 1. Chemical composition of experimental ore samples (wt %).

Sample	SiO_2	Total Fe	Al_2O_3	CaO	MgO
pure quartz	99.20	<0.001	0.67	<0.001	<0.001
Industrial ore	34.86	42.00	1.35	0.69	1.04

The industrial ore used in this bench-scale flotation tests were a magnetic separation concentrates supplied by Sijiaying iron mine, Tangshan, China. The results of chemical compositions and X-ray diffraction (XRD) analyses were shown in Table 1 and Figure 1b. The samples contained 42.00% Fe (TFe) and 34.86% SiO_2 and were mainly composed of quartz, magnetite and hematite.

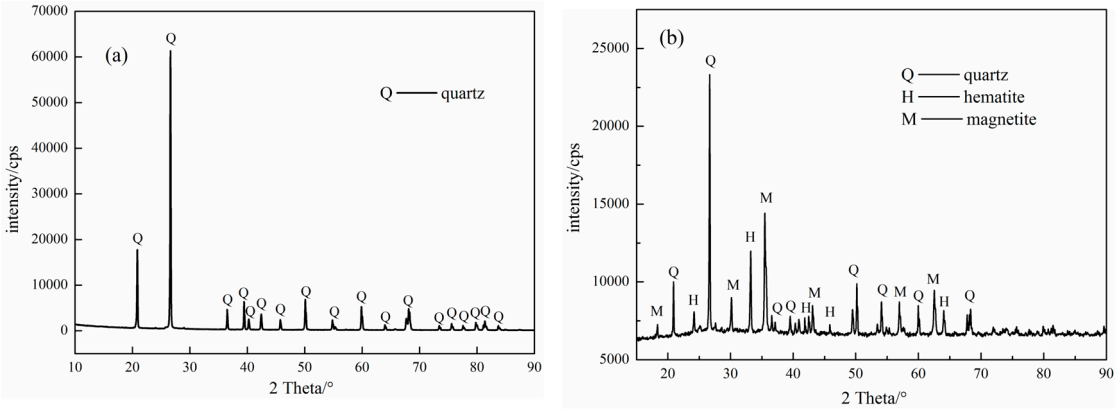

Figure 1. X-ray diffraction patterns of quartz (**a**) and industrial ore (**b**).

2.2. Reagents

The waste cooking oil was provided by Wuhan Zeyu Waterproof Building Materials Ltd., Wuhan, China. The SFA and UFA prepared from the waste cooking oil would be used as flotation collectors. Corn starch provided by Sijiaying iron mine, Tangshan, China, was hydrolyzed by 20% NaOH solution, which was used as flotation depressant of hematite and magnetite. Calcium chloride ($CaCl_2$) with analytical purity was used as activator in the quartz flotation, which was supplied by Tianjin Kemiou Chemical Reagent Co., Ltd., Tianjin, China. Solutions of HCl and NaOH with concentrations of 0.10 mol/L were used to adjust the pH value of the system. Distilled water was used in all tests.

2.3. Preparation of Collector SFA and UFA

The waste cooking oil (500.0 g) was water washed several times and filtered to remove solid impurities and most of the water-soluble impurities to obtain a mixture of fatty acid glycerides. Appropriate amount of NaOH solution (500.0 mL, 40%) was added and heated to 70 °C for 1 h to convert the mixed fatty acid glyceride to the mixed fatty acids sodium. After treated by H_2SO_4 solution (1000.0 mL, 20%) under the reaction temperature of 80 °C for 2 h, 350.0 g mixed fatty acids (MFA) was obtained.

MFA could be separated into SFA and UFA with urea inclusion method [26–28]. The main process shown in Figure 2. The MFA (100.0 g) dissolved in ethanol (600.0 mL, 95%) and heated to 78 °C. After that urea (200.0 g) was added into the reaction system. The mixture was stirred for 1 h, then taken out and allowed crystal precipitation under 0 °C environment for 12 h. In this two-phase system, SFA was wrapped in solid phase crystals and UFA was dissolved in the mother liquor. Finally, both UFA and SFA could be obtained by water dissolving and dispensing. In this study, SFA and UFA were used as the collectors in the pure mineral flotation of quartz after being saponified with 20% NaOH solution in a mass ratio of 1:1.

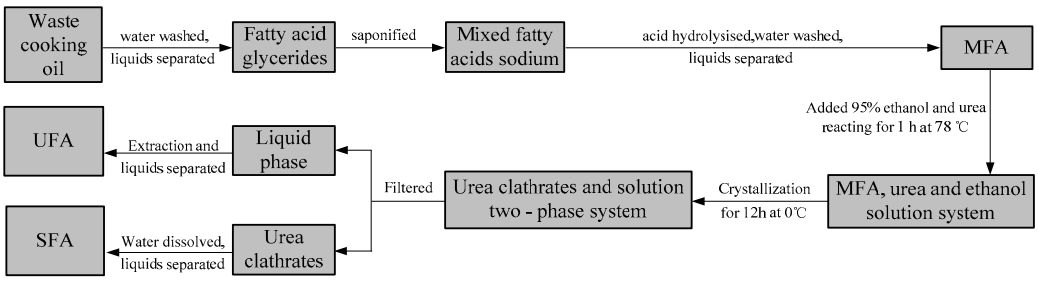

Figure 2. The preparation process of collector SFA and UFA from waste cooking oil.

2.4. Determination of Melting Point and Iodine Value

The melting point of the fatty acid was determined by a DFYF-194 petroleum product freezing point analyzer (DFYF-194, Dalian Analytical Instrument Co., Ltd., Dandong, China). Using anhydrous ethanol as the heat transfer medium, the sample was placed in a clean tube and the temperature was adjusted every 30 min until the sample was solidified. The error in temperature must be kept within 0.2 °C.

The iodine value is the iodine consumption in 100.0 g sample, which is usually used as an indicator of unsaturation degree in an organic compound [29]. For fatty acids, the higher the iodine value is, the greater the degree of unsaturation. In this work, an appropriate amount of sample was taken, dissolved in 10.0 mL carbon tetrachloride and added in 25.0 mL Wechsler's solution (the solution of iodine chloride and glacial acetic acid). After that, the potassium iodide solution (10.0 mL, 20%) was added in and titrated by 0.1 mol/L sodium thiosulfate standard solution. Starch Solution (1.0 mL, 1%) was used as the indicator in titration.

The iodine value of fatty acid was calculated by the following equation:

$$I = \frac{(v_0 - v_1) \times c \times 126.9}{m \times 1000} \times 100 \quad (1)$$

where I is the iodine value of fatty acid, v_0 and v_1 are the consumption volume (mL) of sodium thiosulfate standard solution in blank test and sample test respectively. The c is the concentration (mol/L) of sodium thiosulfate standard solution and m is the quality (g) of the sample taken.

2.5. Fourier Transform Infrared Spectroscopy

The characteristic absorption peaks of the infrared spectra can be used to analyze some structural features of the collector molecules [30]. In the measurement of collectors FTIR, spectral pure KBr was ground to below 0.002 mm and pressed into thin slices with a special mold. The collector UFA or SFA were then dipped to the KBr slice by a glass rod to determine the infrared spectrum by Nicolet 380 FT-IR spectrometer (Nicolet 380 FT-IR, Thermo Fisher Scientific, Waltham, MA, USA).

2.6. Molecular Simulation

The calculations were carried out by Cambridge serial total energy package (CASTEP) (Materials Studio 7.0, NeoTrident Technology Ltd, Shanghai, China), which is a first-principle presudopotential method based on DFT using ultra-soft pseudopotentials [31] and a plane-wave (PW) expansion of the wave functions [32]. In this study, CASTEP module was employed to geometry optimization and property analysis of fatty acid molecules and urea crystals to investigate the separation principle of fatty acids with urea inclusion method.

The exchange-correlation function used was the generalized gradient approximation (GGA), because of its high accuracy in the hydrogen bond description [33]. The interactions between valence electrons and the ionic core were represented with ultra-soft pseudopotentials. The energy cutoff for the plane-wave basis was 340 eV. The DFT-D correction was adopted. The atomic positions were optimized using the Perdew-Burke-Ernzerhof solids (PBESOL) algorithm [34]. The threshold values for the convergence criteria were 0.0001 nm for maximum displacement, 0.3 eV/nm for maximum

force, 0.05 GPa for maximum stress, 1.0×10^{-5} eV/atom for energy and 1.0×10^{-6} eV/atom for self-consistent field tolerance.

2.7. Micro-Flotation

The micro-flotation tests were conducted in a 50 mL flotation cell of a XFGII50 laboratory flotation machine (XFGII50, Jilin Exploration Machinery Plant, Changchun, China) [35]. Taking 5 g quartz samples in the flotation cell filled with ultra-pure water. The pulp was stirred for 3 min at a speed of 1992 rpm. The pH regulator (HCl or NaOH solution), activator $CaCl_2$ and collector (UFA or SFA) were then added into the cell in sequence every 3 min to conduct the flotation for 4 min. Finally, the froth products and tailings were weighed separated after drying and the recovery was calculated based on the weight of the products.

2.8. Bench-Scale Flotation

Bench-scale flotation tests were performed in XFD-63 flotation cell whose volume for rougher flotation was 1.0 L and for cleaner flotation was 0.5 L respectively. The rougher flotation used 300 g industrial ores and the impeller speed was fixed at 1992 r/min. The pulp temperature of bench-scale flotation was maintained at 20 °C (natural pulp temperature). The detailed flotation conditions and the flotation flow sheet of locked cycle tests were listed in Figure 3. Scanning electron microscope with an attached EDS microanalyzer (SEM/EDS) (SSX-550, SHIMADZU, Kyoto, Japan) and X-ray diffraction were used to investigate the characteristics of flotation tailings.

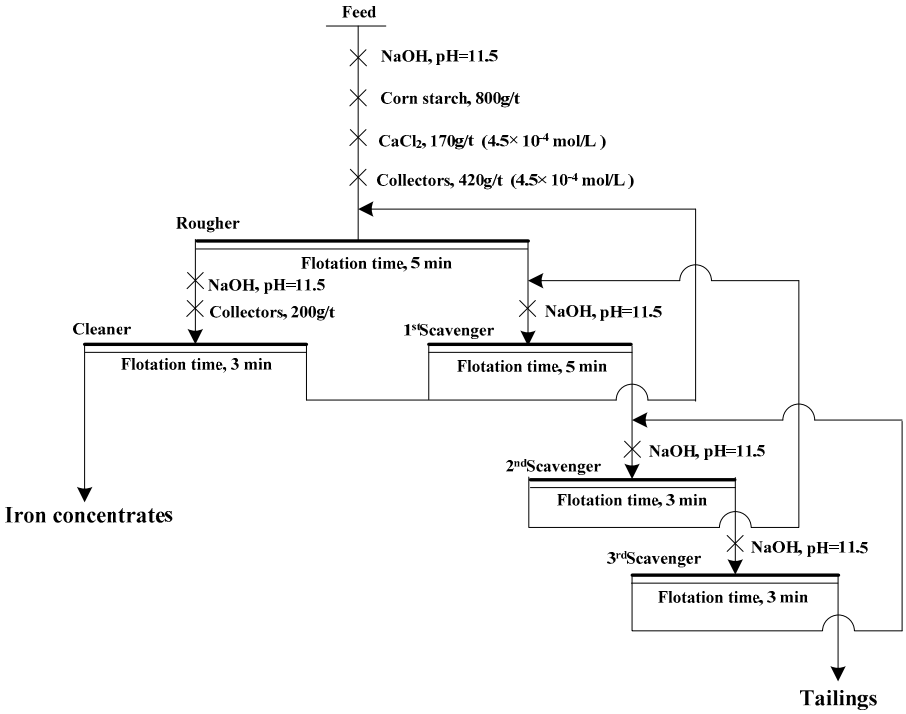

Figure 3. The locked cycle flowsheet of bench-scale flotation.

3. Results and Discussion

3.1. Separation Mechanism of Fatty Acids

Urea was tetragonal crystal structure belonging to the space group P-421M [27]. Urea molecules were connected in a head-to-tail manner to form a straight chain with hydrogen bonds. The planes of adjacent urea chains were almost perpendicular and attracted to each other with hydrogen bonds. The tetragonal crystal structure of urea was shown in Figure 4A.

When the urea and fatty acids to form a urea inclusion compound, the crystal structure of urea was converted from the tetrahedron into hexahedron with a space group of P6122 [26,28]. Urea molecules were in a spiral way to form the host frame structure. The tunnels of this urea host structure could be filled with a dense packing of fatty acids as guest molecules. The results of molecular simulation showed that the diameter of the tunnels in the hexahedral host framework was 0.798 nm. Considering the intermolecular bonding distance, the molecule diameter of the guest fatty acids was 0.35~0.50 nm. The hexagonal crystal structure of urea was shown in Figure 4B.

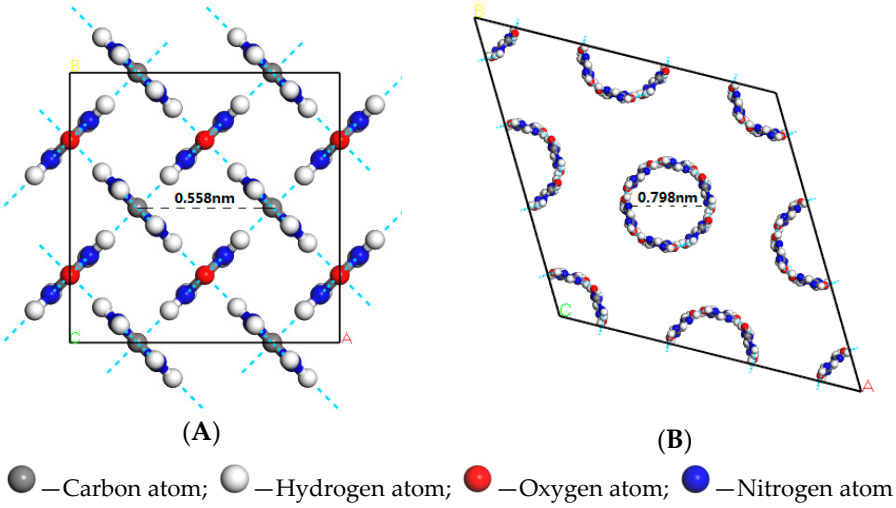

Figure 4. Tetragonal crystal structure (**A**) and hexagonal crystal structure (**B**) of urea.

Quantum mechanics calculations were carried out by Cambridge serial total energy package (CASTEP) based on DFT to optimize the molecular structure of palmitic acid, oleic acid, linoleic acid and linolenic acid in waste cooking oil. The optimized molecular structure of those fatty acids was shown in Figure 5A–D. The calculated molecular width and molecular bending angle were shown in Table 2.

The palmitic acid was a kind of branched saturated fatty acid with a molecular diameter of 0.372 nm. The molecular width of guest fatty acids filled in the tunnels of urea framework should be in the range of 0.35 nm to 0.50 nm, so that the saturated fatty acid molecules could be completely encapsulated in the tunnels of hexahedral urea. For oleic acid, the presence of a double bond (–C=C–) at the ninth carbon atom caused the molecule to bend by 30.53°, resulting in an increase in the molecular width to 0.516 nm. Therefore, the oleic acid could not be completely filled in the tunnels of urea framework. But the part of straight chain containing 9 carbon atoms could be included in the tunnels, when urea was excessive. Due to the existence of two and three (cis) —HC=CH— group, the molecular of linoleic acid and linolenic acid molecules was folded 180 degrees resulting in the width of the molecular more than 0.7 nm, which made linoleic acid and linolenic acid to not be wrapped by urea molecules.

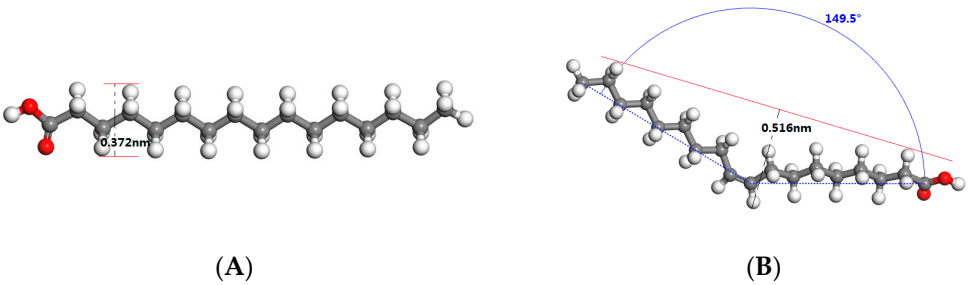

(**C**) (**D**)

Figure 5. Molecular structure of (**A**) Palmitic acid, (**B**) Oleic acid, (**C**) Linoleic acid and (**D**) Linolenic acid in waste cooking oil.

Table 2. Molecular width and molecular bending angle of fatty acid in waste cooking oil.

Fatty Acids	Number of –C=C–	Molecular Width /nm	Molecular Bending Angle/°
Palmitic acid	0	0.372	0
Oleic acid	1	0.516	30.53
Linoleic acid	2	0.766	180
Linolenic acid	3	0.762	180

The quantum mechanics optimization model of complete inclusion of saturated fatty acids and the partial inclusion of oleic acid was shown in Figure 6. In the urea inclusion compound, fatty acids and urea molecules were attracted to each other by hydrogen bonding force to be stable. The blue dashed line between the fatty acid and the urea molecules indicated the hydrogen bond.

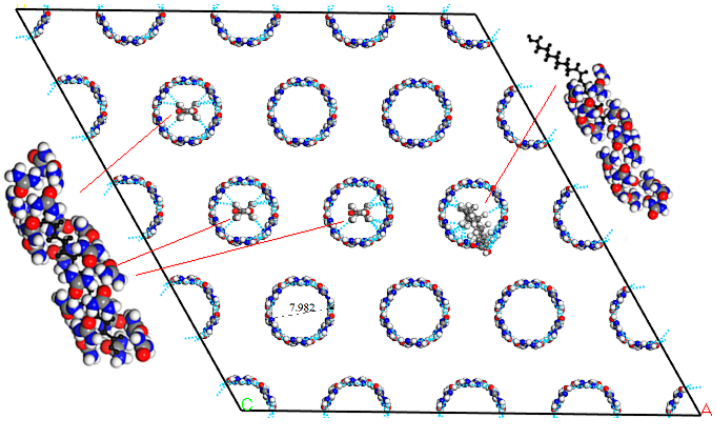

Figure 6. Hexagonal holes framework of urea adduction.

3.2. Characterization of Fatty Acids

The melting point and iodine value of the fatty acids were reported in Table 3. The results showed that the UFA had an iodine value of 162.9, indicating a high degree of unsaturation and its melting point was −17.3 °C, which meant that UFA would possess better dispersibility and solubility at room temperature. Iodine value of SFA was only 49.0, which indicated that SFA was of a low degree of unsaturation and its melting point was up to 38.8 °C. That was to say, SFA must be situated at the temperature above 38 °C in order to achieve proper dissolution and dispersion.

Table 3. Melting point and iodine value of the fatty acids.

Fatty Acids	Yield/%	Melting Point/°C	Iodine Value/(g/100 g)
UFA	64.8	−17.3	162.9
SFA	35.2	38.8	49.0

As shown in the infrared spectrum of UFA (Figure 7), the characteristic peaks at positions of 2922, 2855 and 1464 cm^{-1} assigned to asymmetric stretching of $–CH_3$ group, symmetric stretching and scissoring of $–CH_2$ group [30,36]. The characteristic sharp band at 1709 cm^{-1} was due to the asymmetric stretching of –C=O in the carboxyl group [37]. The absorption peak at 724 cm^{-1} belonged to C–H bending vibration of the methylene chain $–(CH_2)_n–$. The positions of 3009, 1286 and 1090 cm^{-1} come from the typical C–H stretching vibration, outward and inner bending vibration of the (cis) –HC=CH– group [38], respectively. The peak at 2676 cm^{-1} was the vibration absorption peak of $–CH_2$ in $–[HC=CH–CH_2]_n–$ (n > 1) group which was a cumulative carbon–carbon double bond structure [36]. It was indicated that UFA had not only single but cumulative carbon–carbon double bonds, resulting in a higher degree of dissatisfaction. However, the characteristic peaks at positions near 3009, 1286, 1090 and 2676 cm^{-1}, which were assigned to carbon–carbon double bonds and cumulative carbon–carbon double bonds, did not appear in the spectrum of SFA. Therefore, it was proved that in SFA there was no obvious single or cumulative carbon–carbon double bonds. In other words, SFA should be composed of saturated fatty acids.

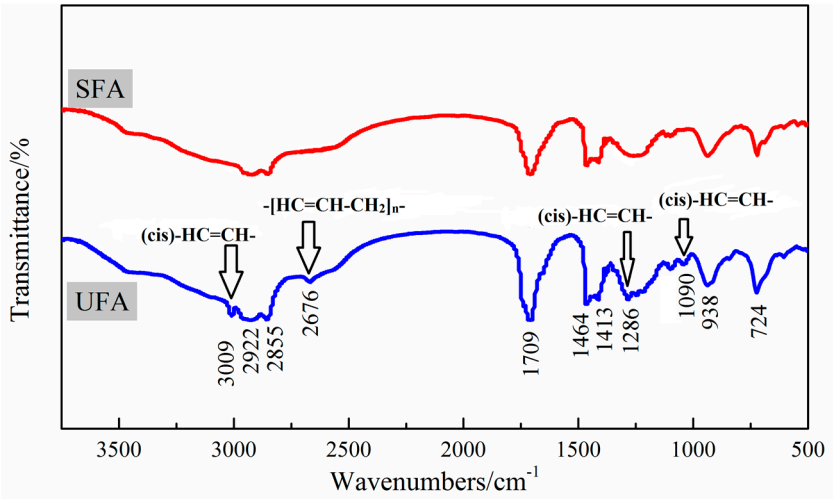

Figure 7. FT-IR spectra of fatty acids.

3.3. Micro-Flotation Tests

Quartz was floated at various pH with collector (UFA or SFA) concentration of 4.5×10^{-4} mol/L and activator $CaCl_2$ concentration of 5×10^{-4} mol/L at 30 °C and the flotation recoveries of quartz were presented in Figure 8A. The results showed that when pH of the pulp was less than 8, flotation recoveries by UFA and SFA were both lower than 20%. When the pH value increased from 8 to 11.5, quartz recovery by UFA and SFA improved to the highest level for 99.32% and 94.01%. Therefore, the optimum pH value for quartz flotation was 11.5. Moreover, UFA presented better collectability than SFA within the whole pH range.

Figure 8B showed the recovery of quartz as a function of concentration of SFA and UFA. The flotation tests were carried out under the conditions of pH 11.50, 5×10^{-4} mol/L $CaCl_2$ as the activator and flotation temperature at 30 °C. Increasing the concentration of UFA from 0.7×10^{-4} mol/L to 3.5×10^{-4} mol/L (point a to point b), the recovery of quartz increased from 47.24% to 99.32%. Upon further increase in the UFA dosage, the quartz recovery remained unchanged. Therefore, the most appropriate dosage of UFA was 3.5×10^{-4} mol/L (point b). For the collector SFA, the quartz recovery reached a highest value of 93.38% at the concentration of 4.5×10^{-4} mol/L (point c), which, in comparison, could be achieved with only 2.3×10^{-4} mol/L (point d) of UFA. Therefore, UFA had obviously the stronger collectability for quartz.

As shown in Figure 8C, the effect of activator $CaCl_2$ on the flotation of quartz was investigated with the collector of UFA and SFA. The collector dosage of UFA and SFA was taken as 3.5×10^{-4} mol/L and 4.5×10^{-4} mol/L with a pulp pH of 11.5 and flotation temperature of 30 °C. The results showed

that SFA was sensitive to activator $CaCl_2$. The flotation recovery of quartz using SFA as a collect rapidly increased from 7.19% to the highest value 93.5% with the increase of the $CaCl_2$ concentration from 0.5×10^{-4} mol/L to 4.5×10^{-4} mol/L. For the collector UFA, the optimum $CaCl_2$ concentration of quartz flotation was only 2.3×10^{-4} mol/L and a flotation recovery 99.7% was obtained. Even dosage of $CaCl_2$ at a very low level of 0.5×10^{-4} mol/L, flotation recovery was still higher than 90%. It was indicated that the activator $CaCl_2$ had little effect on the flotation performance of the collector UFA and the concentration of activator $CaCl_2$ required for the collector UFA was less than that of SFA.

Figure 8D showed the effect of flotation temperature on the performance of collectors (UFA and SFA), under optimal flotation conditions. The results of flotation temperature tests showed that the temperature of the pulp had little effect on the flotation performance of the collector UFA. In the temperature range from 10 °C to 50 °C, the quartz recovery of UFA flotation was above 98%. However, if the same flotation recovery rate was obtained, the flotation temperature for SFA must be higher than 35 °C. Therefore, the collector UFA had performed better at relatively lower temperature than SFA.

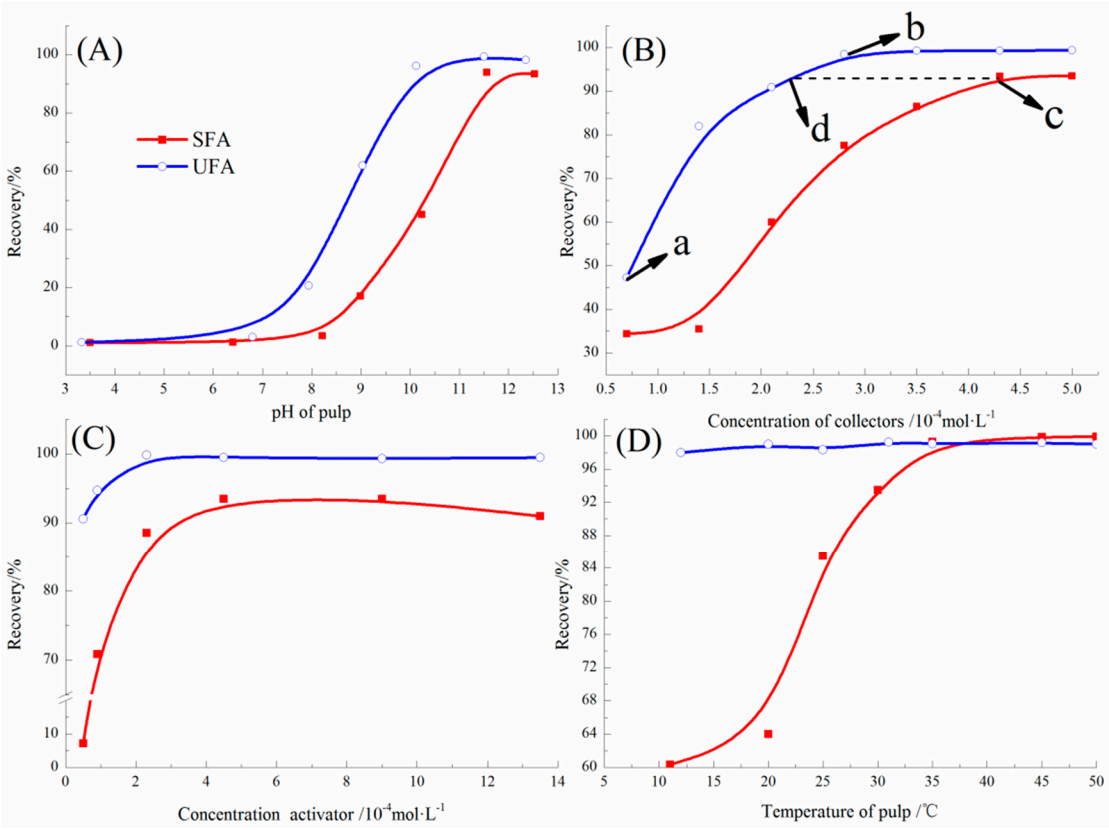

Figure 8. Recovery of quartz as a function of pulp pH (**A**), collector concentration (**B**), activator $CaCl_2$ concentration (**C**) and pulp temperature (**D**) with UFA or SFA.

The micro-flotation results demonstrated that the optimum pH value for quartz flotation was 11.5. Compared with the collector SFA, the collector UFA displayed a superior collecting ability for the flotation of quartz at an extremely low temperature, 10 °C. Besides, the collector UFA also had the advantages of low dosage, wider collector range and calcium ions tolerance. The reason for waste cooking oil having a poor flotation performance when used directly was due to the large amount of SFA in presence.

3.4. Bench-Scale Flotation

Based on the excellent flotation results of micro-flotation tests, bench-scale flotation tests were performed with industrial iron ores to further investigate the flotation performance of UFA and SFA. The flowsheet of bench-scale flotation tests was shown in Figure 3 and flotation results were presented in Table 4.

The results in Table 4 showed that the flotation concentrates with 54.00% TFe and 14.98% SiO_2 could be obtained by using collector SFA and the flotation recovery of TFe was 82.26%. While for UFA, the TFe grade and recovery of its flotation concentrates were 66.58% and 85.42% with 2.26% SiO_2. Therefore, the collecting ability of UFA was further confirmed to be stronger than SFA. The large amount of SFA in presence caused the poor flotation performance of waste cooking oil when used directly.

Compared with the flotation concentrates obtained by using un-separated waste cooking oil (MFA) as collector, the TFe grade and recovery of the concentrates produced by UFA flotation were 4.09 percentage points and 2.70 percentage points higher and the contents of SiO_2 was 4.03 percentage points lower at the same time. Thus, if the SFA in the waste cooking oil was separated out, the flotation performance of the waste cooking oil could be greatly strengthened.

Table 4. Results of bench-scale flotation

Collector	Product	Weight/%	Grade/%		Recovery/%	
			Fe	SiO_2	Fe	SiO_2
SFA	Tailings	36.48	20.28	59.53	17.74	72.72
	Concentrates	63.52	54.00	14.98	82.26	27.28
	Feed	100.00	41.70	34.88	100.00	100.00
UFA	Tailings	45.98	13.35	73.41	14.58	95.98
	Concentrates	54.02	66.58	2.62	85.42	4.02
	Feed	100.00	42.10	35.17	100.00	100.00
MFA (Un-separated)	Tailings	44.12	16.53	70.93	17.28	89.39
	Concentrates	55.88	62.49	6.65	82.72	10.61
	Feed	100.00	42.21	35.01	100.00	100.00

The results of XRD analysis and SEM photomicrographs (with EDS) analysis of the reverse flotation tailings (flotation foam products) obtained by using collector UFA and collector SFA were shown in Figures 9 and 10, respectively. The results showed that the reverse flotation tailings of collector UFA and collector SFA were both mainly composed of quartz and a small amount of hematite and magnetite but the contents of SiO_2 in UFA reverse flotation tailings were higher than that of SFA.

SFA flotation tailings include not only a lot of quartz-iron intergrowths but also a little monomeric iron minerals such as particle a in Figure 10A. However, no monomeric iron minerals had been found in the flotation tailings of collector UFA, indicating that UFA has better collection and selectivity than SFA and UFA was an excellent collector for reverse flotation desilication of iron ores.

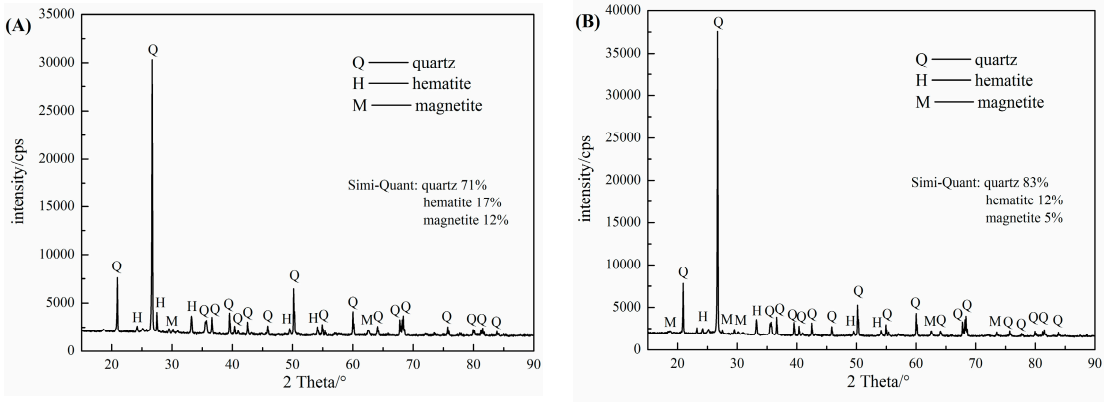

Figure 9. X-ray diffraction of flotation tailings with collector SFA (**A**) or collector UFA (**B**).

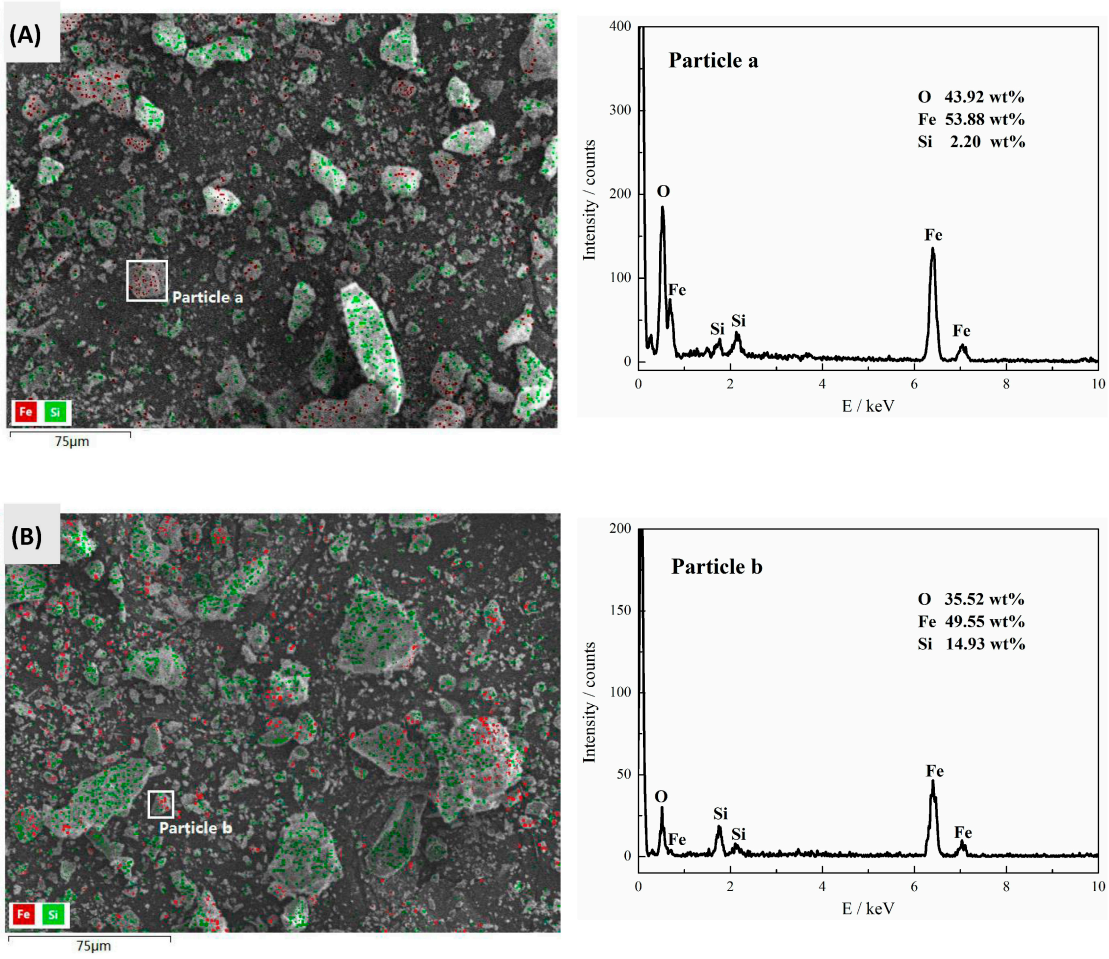

Figure 10. SEM photomicrographs with EDS: (**A**) flotation tailings with collector SFA; (**B**) flotation tailings with collector UFA.

4. Conclusions

Molecular simulation showed that the separation of SFA and UFA could be achieved by urea adduction. In this approach, the mixed fatty acids (MFA) prepared by the waste cooking oil was separated into saturated fatty acids (SFA) with an iodine value of 48.97, a melting point of 38.8 °C and unsaturated fatty acids (UFA) with an iodine value of 162.90, a melting point of −17.3 °C. The infrared spectroscopy analysis showed that SFA was composed of saturated fatty acids while UFA has more single and cumulative carbon-carbon double bonds with a higher degree of unsaturation.

The micro-flotation tests results of quartz showed that SFA had a poor collectability, which required a flotation temperature more than 35 °C. In contrast, the collectability and selectivity of UFA were strong, even at an extremely low flotation temperature (10 °C). The corresponding flotation recovery at 10 °C was as high as 98%. The results of bench-scale flotation tests further proved that UFA was an excellent collector for reverse flotation desilication of iron ores. The micro-flotation bench-scale flotation tests results revealed that the large amount of SFA in presence caused the poor flotation performance of waste cooking oil. If the SFA in the waste cooking oil was separated out, its flotation performance could be greatly strengthened and the TFe grade and recovery of the flotation concentrates would be increased by 4.09 percentage points and 2.70 percentage points, respectively and the contents of SiO_2 was 4.03 percentage points lower at the same time.

Acknowledgments: The authors gratefully acknowledge and appreciate the financial support provided by the National Natural Science Foundation of China (Grant No. 51274056 and 51474055).

Author Contributions: Wenda Guo and Yimin Zhu conceived and designed the experiments; Wenda Guo and Yuexin Han performed the experiments; Wenda Guo and Yihe Wei analyzed the data; Binbin Luo contributed reagents/materials/analysis tools; Wenda Guo wrote the paper.

Conflicts of Interest: The founding sponsors had no role in the design of the study; in the collection, analyses, or interpretation of data; in the writing of the manuscript and in the decision to publish the results.

References

1. Sheinbaum-Pardo, C.; Calderón-Irazoque, A.; Ramírez-Suárez, M. Potential of biodiesel from waste cooking oil in Mexico. *Biomass Bioenergy* **2013**, *56*, 230–238, doi:10.1016/j.biombioe.2013.05.008.
2. Zhang, Y.; Jiang, Y. Robust optimization on sustainable biodiesel supply chain produced from waste cooking oil under price uncertainty. *Waste Manag.* **2017**, *60*, 329–339, doi:10.1016/j.wasman.2016.11.004.
3. Liang, S.; Liu, Z.; Xu, M.; Zhang, T.Z. Waste cooking oil derived biofuels in China bring brightness for global GHG mitigation. *Bioresour. Technol.* **2013**, *131*, 139–145, doi:10.1016/j.biortech.2012.12.008.
4. Lu, F.; Wu, X. China food safety hits the "gutter". *Food Control* **2014**, *41*, 134–138, doi:10.1016/j.foodcont.2014.01.019.
5. Zhang, H.; Ozturk, U.A.; Wang, Q.; Zhao, Z. Biodiesel produced by waste cooking oil: Review of recycling modes in china, the US and Japan. *Renew. Sustain. Energy Rev.* **2014**, *38*, 677–685, doi:10.1016/j.rser.2014.07.042.
6. Albayrak, A.T.; Yasar, M.; Gurkaynak, M.A.; Gurgey, I. Investigation of the effects of fatty acids on the compressive strength of the concrete and the grindability of the cement. *Cem. Concr. Res.* **2005**, *35*, 400–404, doi:10.1016/j.cemconres.2004.07.031.
7. Kou, J.; Tao, D.; Xu, G. Fatty acid collectors for phosphate flotation and their adsorption behavior using QCM-D. *Int. J. Miner. Process.* **2010**, *95*, 1–9, doi:10.1016/j.minpro.2010.03.001.
8. Liu, B.; Wang, X.M.; Du, H.; Liu, J.; Zheng, S.L.; Zhang, Y.; Miller, J.D. The surface features of lead activation in amyl xanthate flotation of quartz. *Int. J. Miner. Process.* **2016**, *151*, 33–39, doi:10.1016/j.minpro.2016.04.004.
9. Duarte, A.C.; Grano, S.R. Mechanism for the recovery of silicate gangue minerals in the flotation of ultrafine sphalerite. *Miner. Eng.* **2007**, *20*, 766–775, doi:10.1016/j.mineng.2007.02.012.
10. Vidyadhar, A.; Hanumantha Rao, K. Adsorption mechanism of mixed cationic/anionic collectors in feldspar-quartz flotation system. *J. Colloid Interface Sci.* **2007**, *306*, 195–204, doi:10.1016/j.jcis.2006.10.047.
11. Filippov, L.O.; Filippova, I.V.; Severov, V.V. The use of collectors mixture in the reverse cationic flotation of magnetite ore: The role of Fe-bearing silicates. *Miner. Eng.* **2010**, *23*, 91–98, doi:10.1016/j.mineng.2009.10.007.
12. Sahoo, H.; Rath, S.S.; Rao, D.S.; Mishra, B.K.; Das, B. Role of silica and alumina content in the flotation of iron ores. *Int. J. Miner. Process.* **2016**, *148*, 83–91, doi:10.1016/j.minpro.2016.01.021.
13. Ejtemaei, M.; Irannajad, M.; Gharabaghi, M. Influence of important factors on flotation of zinc oxide mineral using cationic, anionic and mixed (cationic/anionic) collectors. *Miner. Eng.* **2011**, *24*, 1402–1408, doi:10.1016/j.mineng.2011.05.018.

14. Luo, X.M.; Yin, W.Z.; Wang, Y.F.; Sun, C.Y.; Ma, Y.Q.; Liu, J. Effect and mechanism of siderite on reverse anionic flotation of quartz from hematite. *J. Cent. South Univ.* **2016**, *23*, 52–58, doi:10.1007/s11771-016-3048-6.
15. Luo, X.; Wang, Y.; Wen, S.; Ma, M.; Sun, C.; Yin, W.; Ma, Y. Effect of carbonate minerals on quartz flotation behavior under conditions of reverse anionic flotation of iron ores. *Int. J. Miner. Process.* **2016**, *152*, 1–6, doi:10.1016/j.minpro.2016.04.008.
16. Li, Z.Y. Application of RA-915 collector in Lilou concentrator. *Met. Mine* **2009**, *11*, 209–211. (In Chinese)
17. Lin, X.H.; Lu, P.; Chen, R.H.; Chen, J.; Ma, X.; Lin, B. Preparation and application of a new type of efficient collector RA-315. *Min. Metall. Eng.* **1993**, *13*, 31–35. (In Chinese)
18. Luo, B.; Zhu, Y.; Sun, C.; Li, Y.; Han, Y. Flotation and adsorption of a new collector α-bromodecanoic acid on quartz surface. *Miner. Eng.* **2015**, *77*, 86–92, doi:10.1016/j.mineng.2015.03.003.
19. Jiang, X.; Wang, X.; Xu, H. Using polyoxyethylene reduction the flotation temperature of fatty acid. *Adv. Mater. Res.* **2011**, *233–235*, 1375–1378, doi:10.4028/www.scientific.net/AMR.233-235.1375.
20. Xiao, J.J.; Qiu, Z.M.; Rao, R.; Luo, C.Y.; Huang, W.; He, W.J. Research progress in preparation of new type flotation collectors from waste cooking oil. *Mod. Chem. Ind.* **2015**, *35*, 57–61. (In Chinese)
21. Ma, Y.W.; Xu, D.L. Development and evaluation of anionic collector KA-1 for hematite flotation at room Temperature. *Min. Metall. Eng.* **2014**, *34*, 53–55. (In Chinese)
22. Li, H.X.; Zhao, J.F.; Huang, Y.Y.; Jiang, Z.W.; Yang, X.J.; Yang, Z.H.; Chen, Q. Investigation on the potential of waste cooking oil as a grinding aid in Portland cement. *J. Environ. Manag.* **2016**, *184*, 545–551, doi:10.1016/j.jenvman.2016.10.027.
23. Guo, W.D.; Zhu, Y.M.; Wei, Y.H.; Duan, D.X. Fatty acid collectors' flotation performance strengthen test using urea adduction method. *Met. Mine* **2015**, *44*, 90–94. (In Chinese)
24. Luo, H.H.; Tang, J.J.; Li, C.X.; Wang, Y.Y.; Chen, B.Y. Flotation performance of plant fatty acid on collophanite at normal temperature. *J. Wuhan Inst. Technol.* **2013**, *35*, 17–20. (In Chinese)
25. Luo, H.H.; Li, C.X.; Tang, J.J.; Wang, Y.Y.; Chen, B.Y. Composition and flotation performance of plant acidic oil. *J. Wuhan Inst. Technol.* **2012**, *34*, 21–24. (In Chinese)
26. Wu, M.Y.; Ding, H.; Wang, S.; Xu, S.M. Optimizing conditions for the purification of linoleic acid from sunflower oil by urea complex fractionation. *J. Am. Oil Chem. Soc.* **2008**, *85*, 677–684, doi:10.1007/s11746-008-1245-7.
27. Ilott, A.J.; Palucha, S.; Batsanov, A.S.; Harris, K.D.M.; Hodgkinson, P.; Wilson, M.R. Structural Properties of Carboxylic Acid Dimers Confined within the Urea Tunnel Structure: An MD Simulation Study. *J. Phys. Chem. B* **2011**, *115*, 2791–2800, doi:10.1021/jp110137h.
28. Hayes, D.G.; Van Alstine, J.M.; Setterwall, F. Urea-based fractionation of seed oil samples containing fatty acids and acylglycerols of polyunsaturated and hydroxy fatty acids. *J. Am. Oil Chem. Soc.* **2000**, *77*, 207–213, doi:10.1007/s11746-000-0033-5.
29. Chuah, L.F.; Klemes, J.J.; Yusup, S.; Bokhari, A.; Akbar, M.M. Influence of fatty acids in waste cooking oil for cleaner biodiesel. *Clean Technol. Environ. Policy* **2017**, *19*, 859–868, doi:10.1007/s10098-016-1274.
30. Lima, R.M.F.; Brandao, P.R.G.; Peres, A.E.C. The infrared spectra of amine collectors used in the flotation of iron ores. *Miner. Eng.* **2005**, *18*, 267–273, doi:10.1016/j.mineng.2004.10.016.
31. Vanderbilt, D. Soft self-consistent pseudopotentials in generalized eigenvalue formalism. *Phys. Rev. B* **1990**, *41*, 7892–7895, doi:10.1103/PhysRevB.41.7892.
32. Sun, J.; Wang, H.T.; He, J.L.; Tian, Y.J. Ab initio investigations of optical properties of the high-pressure phases of ZnO. *Phys. Rev. B* **2005**, *71*, 5132, doi:10.1103/PhysRevB.71.125132.
33. Zhu, Y.M.; Luo, B.B.; Suo, C.Y.; Liu, J.; Sun, H.T.; Li, Y.J.; Han, Y.X. Density functional theory study of α-Bromolauric acid adsorption on the α-quartz (101) surface. *Miner. Eng.* **2016**, *92*, 72–77, doi:10.1016/j.mineng.2016.03.007.
34. Ren, Z.J.; Yu, F.T.; Gao, H.M.; Chen, Z.J.; Peng, Y.J.; Liu, L.Y. Selective separation of fluorite, barite and calcite with valonea extract and sodium fluosilicate as depressants. *Minerals* **2017**, *7*, 24, doi:10.3390/min7020024.
35. Liu, R.Q.; Sun, W.; Hu, Y.H.; Wang, D.Z. New collectors for the flotation of unactivated marmatite. *Miner. Eng.* **2010**, *23*, 99–103, doi:10.1016/j.mineng.2009.10.010.

36. Bellamy, L.J. *The Infrared Spectra of Complex Molecules*; Wiley: New York, NY, USA, 1975.
37. Cao, Q.B.; Cheng, J.H.; Wen, S.M.; Li, C.X.; Bai, S.J.; Liu, D. A mixed collector system for phosphate flotation. *Miner. Eng.* **2015**, *78*, 114–121, doi:10.1016/j.mineng.2015.04.020.
38. Zhou, F.; Yan, C.J.; Wang, H.Q.; Sun, Q.; Wang, Q.Y.; Alshameri, A. Flotation behavior of four C18 hydroxamic acids as collectors of rhodochrosite. *Miner. Eng.* **2015**, *78*, 15–20, doi:10.1016/j.mineng.2015.04.006.